 doi:10.20944/preprints202209.0144.v1

Short silk fiber reinforced PETG biocomposite for biomedical applications

Vijayasankar K N,[1] Sumanta Mukherjee,[2] and Falguni Pati[3,] *

[1]Department of Biomedical Engineering, Indian Institute of Technology Hyderabad, Kandi, Sangareddy – 502284, Telangana, India,

[2]BIT Sindri, Dhanbad, Jharkhand, India.

Abstract

Several biomedical products, like scaffolds, implants, prostheses, and orthoses, require materials having superior physicochemical and biological properties. Polyethylene terephthalate glycol (PETG) is being increasingly used for various biomedical applications. There are a few studies on PETG-based composites, however, natural fibers like silk short fibers reinfored PETG composites have not been attempted. Being a cost-effective widely available material, PETG-Silk combination can be potential biocomposite for several biomedical applications. Here, we report a novel short silk fiber reinforced PETG composite prepared by a wet-mixing route, ensuring homogenous dispersion of the filler. Different ratios (2-10%) of short silk fibers were used to prepare composites with varied compositions. The mechanical, physicochemical, and biological properties of the prepared composites were analyzed. Thermogravimetric analysis showed that such composites are thermally stable up to 390 °C and can be used for thermal extrusion-based manufacturing. The tensile modulus of the samples increased with fiber content; however, the failure strain reduced with fiber content. Furthermore, upon annealing, the tensile modulus increased but, the failure strain of the composites decreased, XRD study revealed that heat treatment has altered the crystalline nature of the composites. Finally, we evaluated the cytocompatibility of the prepared composites to assess their suitability for various biomedical applications.

Keywords : Biocomposites (A), Natural fibres (A), Thermomechanical properties (B), Annealing (E), Biocompatibility.

 doi:10.20944/preprints202209.0144.v1

*falguni@bme.iith.ac.in, Contact number

Introduction

Polymer composites are in demand due to their superior properties over individual materials for several biomedical applications like prostheses, orthoses, and implants. Compared to homogenous monolithic materials, polymer composites offer a wide potential of structural biocompatibility. Since, fiber reinforced polymer composite possesses low modulus and high strength, it is widely preferred for orthopedic applications [1][2].Properties of these biocomposites can be tailored to meet the mechanical and physiological requirement of different biomedical structures by controlling the fiber volume fraction and arrangement, fiber particle size and matrix type. PEEK, PCL, PLA, PVC, PC, and PET are some of the commonly used polymer matrices for composite based biomedical structure fabrication [1] [3] [4].

The recent trend in biomaterial research indicates a wide attraction toward Glycol-modified PET (PETG - Polyethylene terephthalate glycol). Compared to semi crystalline PET, PETG has high transparency and strength [5]. Cyclohexane ring present in the structure of cyclohexanedimethanol group of PETG improves thermal stability, mechanical properties and the transparency of the copolymer and helps to remain PETG in amorphous conditions under processing [5][6]. PETG is a popular material used by biomedical engineers because of its high 3D printability. It is also well-suited for injection molding, extrusion, blow molding, and thermoforming [7]. Hence, PETG has got a wide range of applications. For example, prosthetic check sockets fabricated out of PETG performed remarkably better than ThermoLyn rigid, Orfitrans Stiff materials [8][9]. PETG is also treated as an advanced material for occlusion appliances [10]. Another use of PETG is for patient-specific orthopedic

 doi:10.20944/preprints202209.0144.v1

applications such as scoliosis braces and bone scaffolds [11][12]. However, PETG is unsuitable for specific load-bearing applications as Young's modulus, and ultimate strength are low compared to other thermoplastic materials like HDPE and ABS [13] [14].

Though studies report PETG and its potential uses in the medical field, the literature on PETG based composites is limited. PETG based polymer blends, expanded graphite-reinforced, and carbon-fiber-reinforced PETG composites were studied by various researchers [15][16][17][18] . PETG/TPU blends were used to 3D print maxillofacial implants [14]. Poor adhesion of PETG matrix-Kevlar fiber resulted in low interfacial strength in Kevlar-PETG composite [19]. Further, Sander Rijckaert et.al, proposes improving impregnation quality of aramid fiber-PETG composite for enhancing mechanical properties [20]. However, synthetic fibers can be replaced with environmentally friendly, less expensive natural fibers to improve the properties of PETG. Moreover literature on PETG based natural fiber composites is limited. Waste paper PETG composite prepared by processing beyond 190 °C, resulted in reduced tensile and flexural properties due to decomposition of waste paper powder [21]. Presence of bamboo flour agglomerates and interfacial defects resulted in lower flexural strength of bamboo floor PETG composites [22]. Whereas, Silk is one of the abundant natural fibers possessing excellent mechanical properties and has been used as a reinforcement fiber with various thermoplastic matrices. Silk is considered one of the strongest natural fibers [23]. Silk possesses superior properties compared to plant fibers, and its specific mechanical properties are as good as glass fibers. Low density, high strength, toughness, and high elongation at low temperatures were exhibited by silk fibers [24]. Chemically, silk is a natural protein that consists of fibroin and sericin , where sericin is hydrophilic and fibroin is hydrophobic [25]. Hence, we investigate the

 doi:10.20944/preprints202209.0144.v1

preparation of a PETG based biocompatible composite with short silk fibers as reinforcement. Besides, aging may cause earlier failure in some amorphous polymers, and scientific reports on the aging of PETG and its composite are limited [26]. PETG and PETG based composites should be subjected to detailed study, for their extensive use in biomedical applications,

Information on the thermomechanical and mechanical strength of these composites and its response to temperature is also vital for biomedical applications; however, there are not enough studies on these. In this context, we report novel short silk fiber reinforced PETG biocomposite preparation and its detailed thermal, physicochemical, and biological characterizations to understand its properties. Furthermore, thorough mechanical studies were performed to assess the improvement in the mechanical response of the composites upon heat treatment. And finally, the biological response of the prepared composites was measured by cytocompatibility analysis to understand their suitability for biomedical applications.

2. Materials and methods

2.1 Composite Preparation and Annealing

Bombyx mori Silk cocoons (procured from Central Sericulture Research and Training Institute, Mysore, India) were partially degummed using 0.1 M NaOH (Sigma-Aldrich) solution. These fibers were chopped using Grinding Mill (IK, MF10) to an average size 3.71 mm. PETG pellets (Solidspace Technology, Nashik, India) were dissolved in chloroform (Sigma-Aldrich), and the silk fibers were added in small quantities at a time to prepare composites with 2%, 5%, and 10% (by weight) reinforcement. The solutions were sonicated to disperse the fibers in the matrix using an ultrasound sonicator. Silk-PETG film was prepared by solvent evaporation and subsequent casting in a Petri dish

Preprints (www.preprints.org) | NOT PEER-REVIEWED | Posted: 12 September 2022 doi:10.20944/preprints202209.0144.v1

and overnight drying, obtained films were subsequently dried in vacuum for 24 hours to remove residual solvent. Pure PETG film (0%Silk-PETG), PETG-Silk composite films of 2%, 5%, and 10% weight of silk fibers (2%Silk-PETG, 5%Silk-PETG, 10%Silk-PETG) were characterized and analyzed. All samples were annealed at 57 ℃ (20 ℃ less than the glass transition) by keeping the samples in an oven set at a temperature less than the glass transition temperature of PETG for 30 h and subsequently cooled for 2 h.

2.2 Thermal Characterization

2.2.1 Thermogravimetric Analysis (TGA)

Thermal degradation of samples was analyzed by thermogravimetric analysis. Perkin Elmer (STA 6000, USA) was used for analyzing all the samples. All samples were heated from 30 °C to 650 °C at a 10 °C/ min rate in an inert atmosphere.

2.2.2 Differential Scanning Calorimetry (DSC)

The crystallization trend and melting temperature of the samples were studied using a differential scanning calorimeter (TA DSC 250, USA). All samples were heated from 30 °C to 200 °C at 10 °C/min to eliminate thermal history, and then cooled to 30 °C at 10 °C/min. Second heating cycle was performed from 30 °C to 400 °C at a rate of 10 °C/min under nitrogen atmosphere. Analyses were carried out in closed crucibles with an empty crucible as reference.

2.3 Dynamic Mechanical Analysis

DMA is conducted on a Q800 analyzer (TA Instruments, USA) to understand the viscoelastic behavior of the composites, such as storage modulus and loss modulus under tension. The dimension of the test specimens was 40 × 3 × 1 mm^3 (length × width × thickness). The samples were tested at 1 Hz frequency and at a heating rate of 2 °C/min. Tests were carried out from 25 °C to 150 °C.

Preprints (www.preprints.org) | NOT PEER-REVIEWED | Posted: 12 September 2022 doi:10.20944/preprints202209.0144.v1

2.4 Fourier Transform Infrared Spectroscopy

FTIR spectrometer (Thermo scientific Nicolet iS5, USA) was used for FTIR analysis. Each sample was scanned over the frequency range of 4000– 400cm^{-1} and 32 times at the resolution of 2 cm^{-1}.

2.5 X-ray Diffraction Analysis

The crystallinity of the samples was analyzed by X-ray Diffraction (Rigaku, ultima 4, Japan). All samples were scanned for a 2Θ of 0°- 40° similar to references [27] [28], using Cu Kα radiation (k 5 1.5418 A°) at 40 kV and 100 mA at a rate of 10 °/minute. Peaks were deconvoluted using OriginPro9 software with a Gaussian peak function [29].

2.6 Water absorption test

To understand the water absorption rate of the composites experiment was conducted as per ASTM D570-98 standard test method for moisture absorption of plastics. Samples of size 60 × 60 × 1 mm were dried at 50 °C hours for 24 h and were immersed in distilled water for 24 h. Dry weight (M_0) and wet weight after immersion (M_1) of the samples were measured and percentage water absorption (M_t) was calculated as per Eq. (1).

$$M_t(\%) = \frac{M_1 - M_0}{M_0} \qquad (1)$$

2.7 Mechanical testing

Mechanical testing of the samples was performed as per ASTM D1708 under a crosshead velocity of 10 mm/min. Six samples for each group were tested in Universal Testing Machine (Instron, 3367, USA).

2.8 Optical Microscopy and Fiber length measurement

The surface morphology of the composite samples was evaluated by Keyence digital microscope (VHX 6000, Japan). The length was measured using CurveAlign V4.0 Beta software supported by MATLAB MCR 8.4 version. The optical microscopic images

Preprints (www.preprints.org) | NOT PEER-REVIEWED | Posted: 12 September 2022 doi:10.20944/preprints202209.0144.v1

were used for the characterization of fiber length. Fiber length quantification was performed using the CT-FIRE function designed to compute the fiber features. An equal area of ROI has been selected from the images for computing. Later, the pixel data was converted to millimetres by comparing the pixels with the known distance from the scale bar, and the graphs were plotted.

2.9 Scanning Electron Microscopy

The surface of the film and fracture surface of the tensile-tested samples was observed by scanning electron microscope under an accelerated voltage of 1.5 KV on (JEOL JSM-7800F, Japan) FE-SEM.

2.10 Biocompatibility analysis

Biocompatibility of the material was assessed by the metabolic activity of cells on days 1, 7, and 14 using MTT assay (Himedia, cat no. CCK003-1000, India). The metabolic activities of the L929 murine fibroblast cells was used to assess the cytotoxicity by forming formazan dye produced by the reaction of enzymes from the active cells with the tetrazolium salt in the MTT reagent. The formazan crystals formed on the surface of the material and tissue culture plate control were dissolved in dimethyl sulfoxide. The absorbance was measured using a plate reader (PerkinElmer EnSpire, USA) at 560 nm (n = 3).

3. Results and Discussions

3.1 Preparation of the composite

Degumming of the silk cocoons is the first step used to prepare the short silk fiber as the silk has sericin on the outer surface and is mostly hydrophilic. When we tried to mix short silk fiber without degumming in a hydrophobic thermoplastic like PETG, there was no proper bonding between the matrix and the short silk fiber. On the other hand, silk fibroin is mainly hydrophobic and gets well mixed with PETG. Hence, we have

Preprints (www.preprints.org) | NOT PEER-REVIEWED | Posted: 12 September 2022 doi:10.20944/preprints202209.0144.v1

used degummed silk for mixing with the PETG. Furthermore, to maintain the homogeneity of the short silk fiber within the PETG matrix, we have used a wet mixing technique with the help of chloroform. When tried to mix the short silk fiber with PETG matrix by a twin screw extruder without any solvent like chloroform, the short silk fibers tend to form aggregates, and it was challenging to maintain homogeneity.

We successfully prepared short silk fibers reinforced PETG composites with various percentages (2, 5, and 10%) of short silk fibers (Table 1).

Table 1. Sample details and abbreviations used

Sample Name	**Silk Content (Weight percentage)**	**PETG content (Weight percentage)**	**Annealed sample**
0% silk-PETG	0	100	0% silk-PETG*
2% silk-PETG	2	98	2% silk-PETG*
5% silk-PETG	5	95	5% silk-PETG*
10% silk-PETG[1]	10	90	10% silk-PETG*

3.1 Surface Morphology by Optical Microscopy

The elastic modulus and the strength of fiber-reinforced polymer composites are highly influenced by the content, stiffness, length, and orientation of the fibers [30]. Optical microscopic results help for a better understanding of fiber distribution and dispersion. The maximum no. of fibers is falling in the 4 - 8 mm range in raw silk fibers (Fig. 1c); however, there are no fibers present in the range above 2 mm in composites (Fig. 1d). Since, accoustic cavitation is the basic principle behind sonicaton and it is often used to prepare ultra short fibers [31]. Sonication can impart both chemical and physical

Preprints (www.preprints.org) | NOT PEER-REVIEWED | Posted: 12 September 2022 doi:10.20944/preprints202209.0144.v1

repercussions to polymers. Hence, it can be concluded that the composite preparation technique has induced significant fiber breakage and damage .

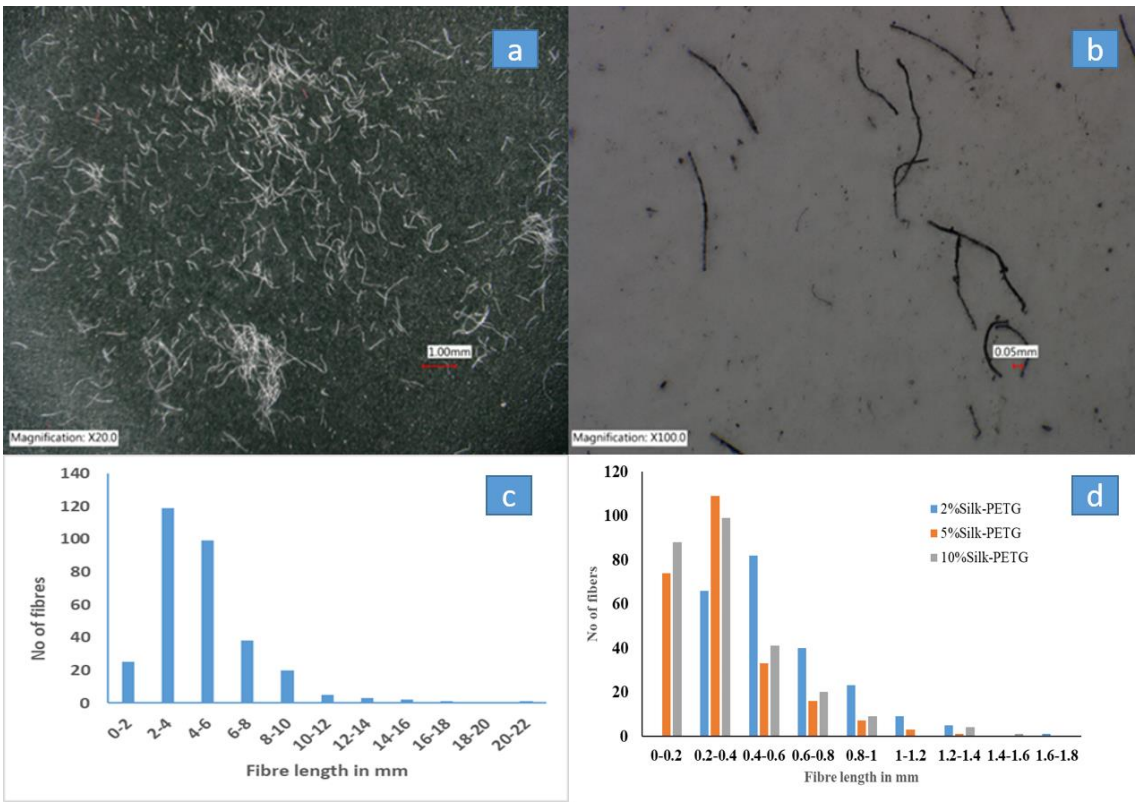

Figure 1. Microscopic images of silk fibers (a & b), c) Fiber length distribution, d) Fiber length in composite

3.2 Thermal Behavior of the Composite

Thermal stability of the prepared composites was studied by thermogravimetric analysis (TGA). Fig. 2a shows TGA curves of silk, pure PETG, and composites. Silk is found to be thermally stable till 295.71 °C and decomposes after 350 °C which is in accordance with the reports published elsewhere [32][33]. In contrast, pure PETG is found to be thermally stable until a temperature of 392.21 °C and also in accordance with other reports [34]. Significant weight loss occurred after 392.21 °C, for both pure PETG and composites, which can be mainly due to degradation of materials, as shown in Fig. 2a. At the same time, weight residue for 10% silk-PETG after 450 °C is high, compared to

 doi:10.20944/preprints202209.0144.v1

pure PETG which could be due to the char formation on the addition of heat resitant silk fibers [33].

Pure PETG and the composites have revealed a single glass transition temperature (Tg) of 77 °C (Fig. 2b). The addition of silk fibers, which have a higher Tg, does not increase the Tg of composites. Increase in Tg implies that more energy is required for processing the composites [35]. The stiff and bulky glycol group does not allow the molecular chain reordering in PETG [36]. This may be the reason for the absence of visible melting or crystallization peak in DSC (Fig. 2b) which is in accordance with similar studies [37].

Dynamic mechanical study reveals the viscoelastic behavior of the composite under varying temperature and constant frequency (Fig. 3a and 3b). In Fig. 3a, Storage modulus continuously decreases at high temperatures, as in the case of thermoplastics. As can be observed, only PETG film has the lowest value of storage modulus at low temperatures. As the fiber content increases, the storage modulus also increases, which can be attributed to the stiffening effect of fiber with matrix or restricted polymer chain movement. Also, it can be due to the effective stress transfer between the fiber-matrix interface [38]. It is also interesting to note that after the glass transition temperature, the decrease in the storage modulus is less for 5% and 10% silk-PETG composites than 0% and 2% silk-PETG composites. It implies that increasing fiber content makes the composite suitable for use at elevated temperatures. Besides fiber content, fiber length also influences the storage modulus of fiber-reinforced composites [39]. If the storage modulus depicts the energy absorbed or stored by composite material, the loss modulus or viscous modulus is a measure of energy dissipated in the form of heat during deformation. At room temperature, the highest loss modulus values are found for only PETG and 2% Silk-PETG composite. At elevated temperatures, loss modulus value

Preprints (www.preprints.org) | NOT PEER-REVIEWED | Posted: 12 September 2022 doi:10.20944/preprints202209.0144.v1

increases with fiber content (Fig. 3b). Maximum heat dissipation occurs at higher values of loss modulus, indicating that an increase in fiber content increases the fiber-matrix interface area and thus friction between matrix and fiber. Interestingly, the loss modulus of 10% Silk-PETG composite increased till 44 °C and then decreased. This can be due to the limited molecular mobility of the PETG matrix at lower temperatures.

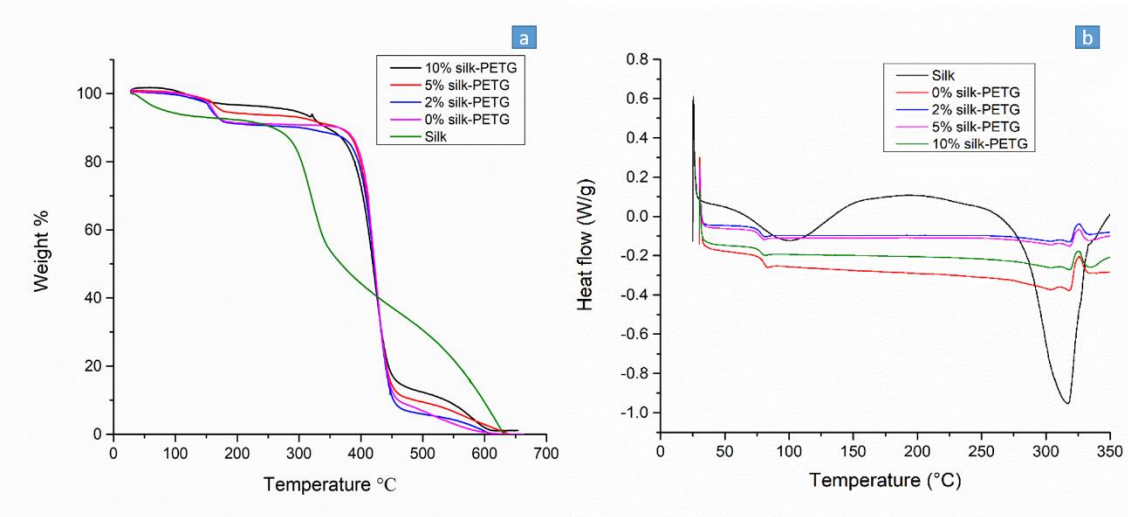

Figure 2. a) TGA, b) DSC plots of the pure PETG, and 2%, 5%, and 10% silk-PETG composites

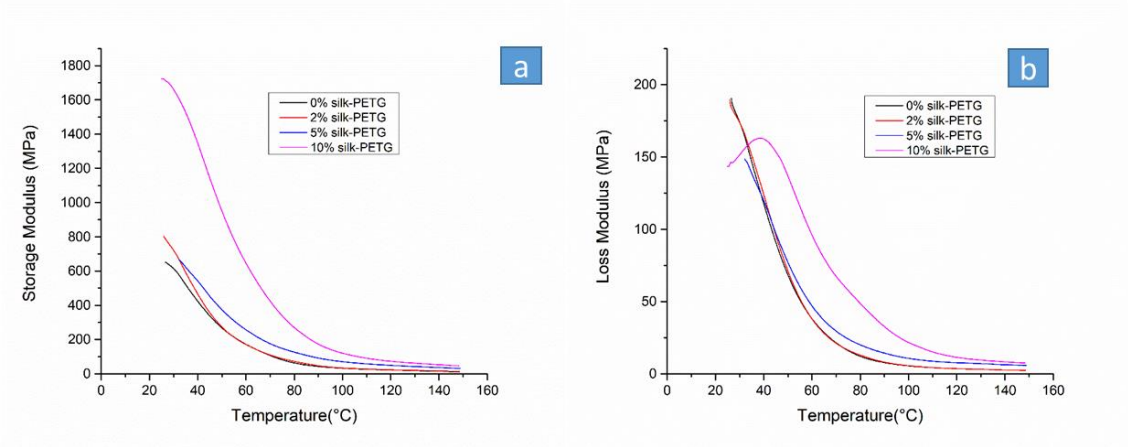

Figure 3. a) Storage Modulus, b) Loss Modulus of the pure PETG, and 2%, 5%, and 10% silk-PETG composites

3.3 FTIR study

Preprints (www.preprints.org) | NOT PEER-REVIEWED | Posted: 12 September 2022 doi:10.20944/preprints202209.0144.v1

To find the possible interaction between fiber and matrix and the presence of silk in composites, FTIR studies have been performed. In Fig 4, C-H stretching bands 3290 $cm^{-1}$and N-H bands at 3274 cm^{-1} were present in the case of silk , which are the most common functional group in silk fibers. Amide I peak present in silk at 1619 cm^{-1} got shifted in composites to 1578 cm^{-1} in 2%,5%,10%Silk reinforced PETG composites, which confirms the presence of silk in prepared composites. Alkenes (C=C) out of plane bend was seen with a high-intensity peak at 722-723cm^{-1}. Peaks which are present from 3000-2800 cm^{-1} representing aliphatic C-H stretching vibrations and these do not show any variations even in reinforced samples. Absorbance peak at 1711-1710 cm^{-1} shows C=O of the ester group of PETG molecule and peaks from 956 to 969 cm^{-1} represent C-H stretching of cyclohexylene ring of PETG [40].

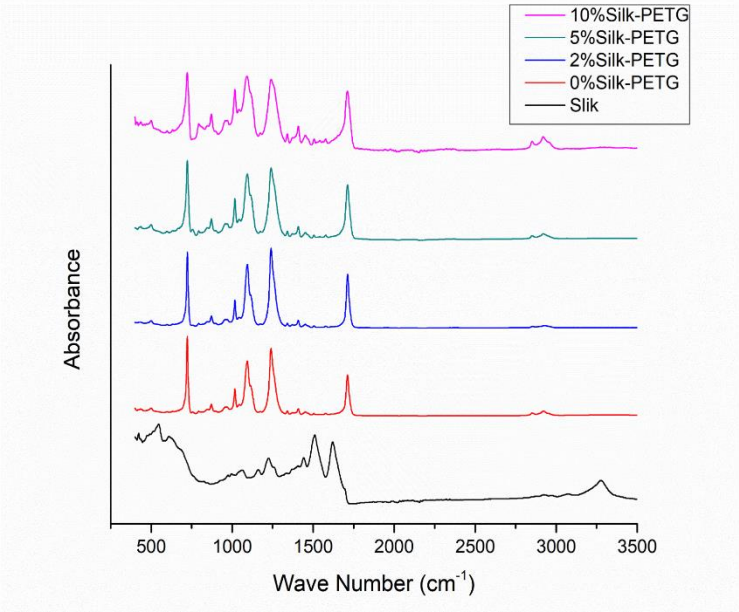

Figure 4. FTIR analysis of the pure PETG, and 2%, 5%, and 10% silk-PETG composites

3.4 XRD Analysis

In the XRD data for the pure silk material, a strong peak was observed at the two-theta value of 21°, and a shoulder peak was present at 25° (Fig.5a), both of which can be

 doi:10.20944/preprints202209.0144.v1

attributed to the typical characteristic peaks for silk. Although no XRD peaks were observable for the pure PETG sample indicating its amorphous nature, some characteristic features were evident in the XRD spectra of all the composites and the annealed specimens. The spectra were deconvoluted for further analysis (Fig.5c-5d)., and peaks were observed at the two-theta values of 17.26° and 20.36°. Both the intensity and the sharpness of the peak at 17.26° increased with increasing silk content.Such changes in the spetra indicate formation and growth of ordered phases in the PETG. Presence of silk in polymer composites has been shown to induce crystallinity in other amorphous polymers like PVA and PVA/PVP, and our results also agree with those observations [41] [42]. Radhakrshnan and Nandkarni [43] have noted crystalline peaks for annealed PETG at 17.4° and 21.95° locations (fig. 5b), which are also present in our data. So, it can be concluded that both the addition of silk and annealing of the composite helped to induce formation and growth of ordered phases in the native amorphous structure of PETG. Silk, which has 50-60% crystallinity in silk fibroin of silkworm B.Mori, may act as a nucleating agent and improves the crystallization ability of the composites as a result of polar interaction of silk with the matrix [44][45][46].

As mentioned before, each fiber consists of fibroin surrounded by sericin. The highly oriented and crystalline structure of Silk II is the reason for the hydrophobicity of silk fibroin and its mechanical strength [44]. Even though in this work, we have degummed silk fibers before mixing to remove hydrophilic sericin. There can be some affinity towards moisture. Our results show that the fiber content increases the water absorption. The higher fiber mass in the 10% silk-PETG sample significantly absorbed more water than pure PETG or sample without silk (Table 2). The result also shows that the addition of silk fiber increases the water absorption significantly disrespect of fiber

Preprints (www.preprints.org) | NOT PEER-REVIEWED | Posted: 12 September 2022 doi:10.20944/preprints202209.0144.v1

content. From the literature, we understood that the water absorption behavior of silk – and polar thermoplastic material matrix composites are not explored to the fullest [13]. The effect of water absorption on the mechanical properties of these composites can be of particular interest [13].

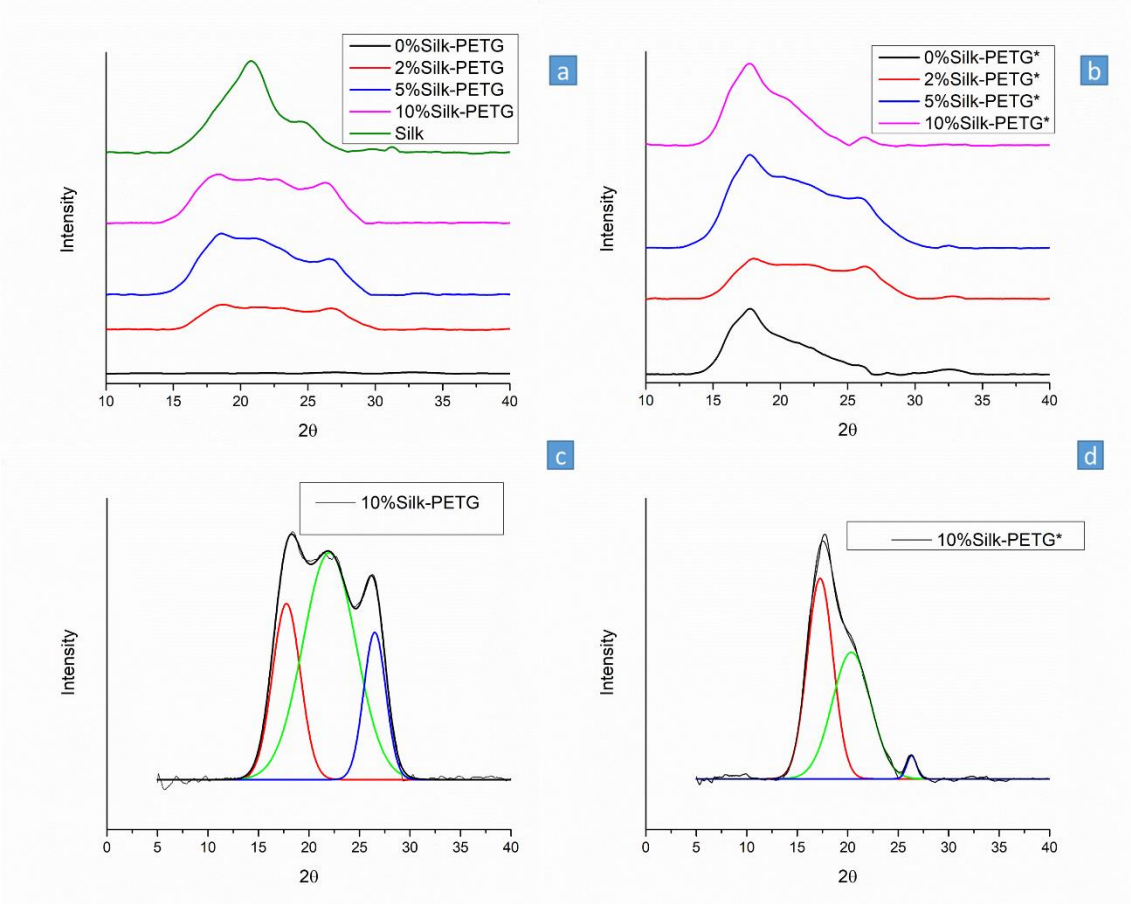

Figure 5. a) XRD analysis of the pure PETG, and 2%, 5%, and 10% silk-PETG composites, b) annealed composites, and deconvoluted XRD patterns of c) annealed 10% Silk-PETG, d) non annealed 10% Silk-PETG.

Preprints (www.preprints.org) | NOT PEER-REVIEWED | Posted: 12 September 2022 doi:10.20944/preprints202209.0144.v1

3.5 Mechanical properties

The thumb rule in fiber-reinforced composite preparation is a brittle fiber-ductile matrix system. Ideally, fibers should have lower failure strain and stiffness; on the other hand, the matrix should have higher failure strain and lower stiffness. Since silk fibers are ductile compared to conventional polymer matrices, it can form a ductile fiber-brittle matrix system. So this may lead to difficulty in using these composites for toughness applications [47]. But it is clear from the mechanical testing result (Fig. 6a) that toughness can be improved with the addition of silk fibers. Annealing significantly alters the mechanical properties of the composite. Mechanical test results elucidate that selective addition of silk fiber in PETG matrix would help to modulate the properties, and hence these composites can be judiciously used for practical applications. As a shortcoming, it is also to be noted that, as Valentini *et al.* [30] stated, silk fibers taken from different parts of the cocoons possess different properties. From Fig. 6b, it is clear that the addition of silk fiber significantly increases the tensile modulus of the composite. Even though the addition of silk fibers results in increased tensile strength in

Table 2. Water absorption analysis of the pure PETG and composites

Sample name	Percentage water absorption	SD	P value (significant difference between dry weight and wet weight)
Pure PETG	0.2147	0.04535	0.091
2% silk-PETG	0.6017	0.2598	0.001
5% silk-PETG	0.8883	0.3467	0.003
10% silk-PETG	2.6433	0.135	0.018

5% Silk-PETG and 10% Silk-PETG composites, the tensile strength of 2% Silk-PETG was found to be lower than that of pure PETG (Fig. 6c), this could be because a smaller number of silk fibers oriented in the direction of loading in 2% Silk-PETG composite.

Preprints (www.preprints.org) | NOT PEER-REVIEWED | Posted: 12 September 2022 doi:10.20944/preprints202209.0144.v1

As the proportion of matrix or Pure PETG in the composite decreases, elongation at break decreases (Fig. 6d). It can be read from the results that more rigid silk fibers do not contribute much to the tensile elongation of the composites.

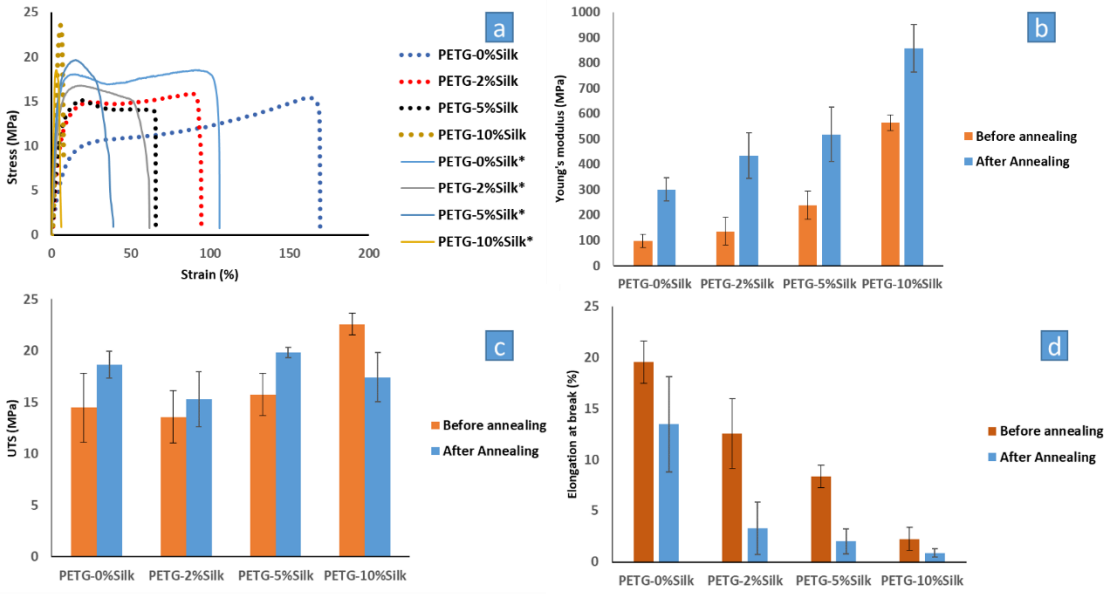

Figure 6. a) Stress-Strain curve, b) Young's Modulus, c) Ultimate tensile strength, d) Elongation at break of the pure PETG and different ratios of silk-PETG composites

3.6 Effect of annealing on the mechanical properties of the composite

We can explicitly argue that annealing influences the mechanical properties of the silk reinforced PETG composite and the pure PETG. Tensile modulus of the composites and pure PETG was found to be increased after annealing. This could be due to the improved interfacial bonding on annealing. At the same time, it is interesting to note that the effect of annealing on tensile strength shows variable response (Fig 6c). In the case of 10% Silk-PETG, tensile strength decreases on annealing. Another interesting observation is that 5% Silk-PETG has increased tensile strength than the pure PETG on annealing. Hence it can be concluded that annealing has improved the tensile strength of 2%, 5%, 10% silk fiber-reinforced PETG composites and pure PETG. Furthermore, failure strain decreases after annealing for composites except for 10% Silk-PETG.

Preprints (www.preprints.org) | NOT PEER-REVIEWED | Posted: 12 September 2022 doi:10.20944/preprints202209.0144.v1

Though, overall result shows that both fiber loading and heat treatment significantly influences the mechanical property. Effect of heat treatment on silk-PETG composites need to be studied in depth to comment further on load transfer and interfacial bonding.

3.7 Failure surface morphology

SEM images of the failure surface reveal more details of the fiber-matrix interactions. After the tensile test, matrix cracks or voids were not present on the surface of pure PETG and 2% Silk-PETG composite. Matrix cracks were present on the 5% Silk-PETG and 10% Silk-PETG composites (Fig7a-7d). Apart from this, no distinct surface textures were found on pure PETG and Silk-PETG composites. It is also can be seen that there is no fiber debonding occurred. No significant trace of a matrix is found on the fibers after failure, which indicates that the fiber-matrix interaction could be improved further. Fiber necking was also visible (Fig. 7f). Relatively increased elongation of 2% Silk-PETG could be due the elongation of both matrix and fiber. Fiber breakage also can be seen in Fig. 7f. More cracks in the matrix were found in 10% Silk-PETG composite, and it can be due to the lack of fiber wetting (Fig. 7h). The absence of fiber breakage in the composites asserts the trend in increasing tensile strength and marks effective load transfer at the interface. It is also to be noted that there are no voids present in the composite, which indicates adequate mixing and dispersion. Furthermore, SEM images reveal no fiber agglomerates present in our composites. Nevertheless, dispersion could be improved further. Surface treatment techniques for natural fibers are widely used for enhancing fiber-matrix bonding and dispersion. Waste paper powder modified with alkyl-ketene-dimer was found to have better dispersion in the PETG matrix [21].

Preprints (www.preprints.org) | NOT PEER-REVIEWED | Posted: 12 September 2022 doi:10.20944/preprints202209.0144.v1

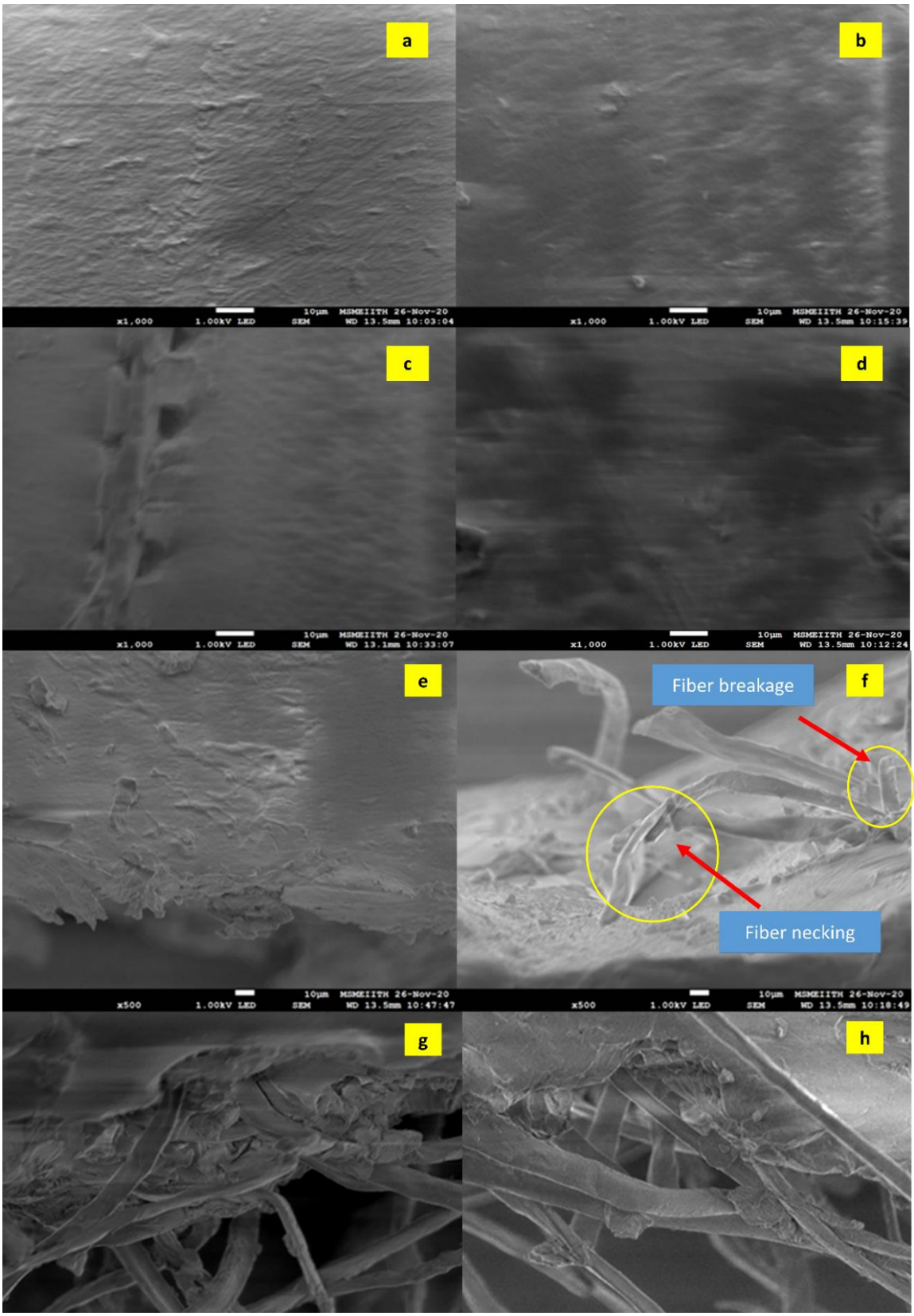

Figure 7. SEM images of composites, surface morphology a) 0% silk-PETG, b) 2% silk- PETG, c) 5% silk-PETG, d) 10% silk-PETG, Failure surface e) 0% silk- PETG, f) 2% silk- PETG, g) 5% silk-PETG, h) 10% silk-PETG

Preprints (www.preprints.org) | NOT PEER-REVIEWED | Posted: 12 September 2022 doi:10.20944/preprints202209.0144.v1

3.8 Biocompatibility analysis

The metabolic activity of cells attached to the composite matrix aids in scrutinizing the cytocompatibility of the prepared composite. The material PETG and different percentages of the silk-PETG composite were found to be non-cytotoxic (Fig. 8). Furthermore, the addition of silk has improved cell adhesion, indicative of the cell-friendly nature of the materials (Fig. 8). We also compared the results with tissue culture plate (TCP) in which we do cell culture, a standard method of culturing cells. The cell number was getting declined or no change on day 14 in all conditions. This is expected to be due to the cell confluence on samples and no space is available for further growth. Comparable results were shown in similar studies where PETG being identified as a bone scaffold material that is cytocompatible and showing cell attachment and proliferation [12] . Hence it can be concluded that the prepared composites are biocompatible and can be used for the biomedical application.

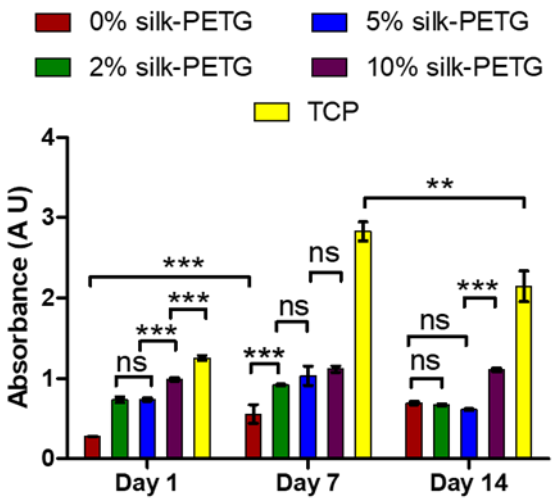

Figure 8. Metabolic activity of the cells attached to the pure PETG and different ratio of silk-PETG composites

4. Conclusions

We have successfully prepared short silk fiber reinforced PETG composite using a wet mixing route. The short fibers were homogenously dispersed within the PETG matrix.

 doi:10.20944/preprints202209.0144.v1

The thermal stability of silk and composites reveals that melt extrusion can be performed without thermal degradation of fiber and matrix. Single glass transition temperature was observed for all composites. Although, XRD study does not show a significant increase in crystallinity on addition of silk fibers, composites revealed an increase in tensile modulus on both fiber addition and annealing . Altogether, the result shows that the prepared composite is biocompatible and may be useful for different biomedical applications.

Acknowledgment

The authors would like to acknowledge the funding support from the MHRD, Gov. of India, and DiponED BioIntelligence, Bangalore, India, for the UAY grant (F.No.21/2015-TS.II/TC, Project No. 35).

References

[1] J. Chen, W. Shi, A.J. Norman, P. Ilavarasan, Electrical impact of high-speed bus crossing plane split, IEEE Int. Symp. Electromagn. Compat. 2 (2002) 861–865. https://doi.org/10.1109/isemc.2002.1032709.

[2] D.K. Rajak, D.D. Pagar, P.L. Menezes, E. Linul, Fiber-reinforced polymer composites: Manufacturing, properties, and applications, Polymers (Basel). 11 (2019). https://doi.org/10.3390/polym11101667.

[3] S. Mohan Bhasney, K. Mondal, A. Kumar, V. Katiyar, Effect of microcrystalline cellulose [MCC] fibres on the morphological and crystalline behaviour of high density polyethylene [HDPE]/polylactic acid [PLA] blends, Compos. Sci. Technol. 187 (2020) 107941. https://doi.org/10.1016/j.compscitech.2019.107941.

[4] X. Li, C. Chu, L. Zhou, J. Bai, C. Guo, F. Xue, P. Lin, P.K. Chu, Fully degradable PLA-based composite reinforced with 2D-braided Mg wires for orthopedic implants, Compos. Sci. Technol. 142 (2017) 180–188. https://doi.org/10.1016/j.compscitech.2017.02.013.

[5] S.R. Turner, Y. Liu, Chemistry and Technology of Step-Growth Polyesters,

Elsevier B.V., 2012. https://doi.org/10.1016/B978-0-444-53349-4.00143-6.

[6] Y.C. Feng, H. Zhao, T.H. Hao, G.H. Hu, T. Jiang, Q.C. Zhang, Effects of poly(cyclohexanedimethylene terephthalate) on microstructures, crystallization behavior and properties of the poly(ester ether) elastomers, Materials (Basel). 10 (2017). https://doi.org/10.3390/ma10070694.

[7] T. Chen, J. Zhang, H. You, Photodegradation behavior and mechanism of poly(ethylene glycol-co-1,4-cyclohexanedimethanol terephthalate) (PETG) random copolymers: correlation with copolymer composition, RSC Adv. 6 (2016) 102778–102790. https://doi.org/10.1039/c6ra21985c.

[8] M.J. Gerschutz, M.L. Haynes, D.M. Nixon, J.M. Colvin, Tensile strength and impact resistance properties of materials used in prosthetic check sockets, copolymer sockets, and definitive laminated sockets, J. Rehabil. Res. Dev. 48 (2011) 987–1004. https://doi.org/10.1682/JRRD.2010.10.0204.

[9] M.J. Gerschutz, M.L. Haynes, D. Nixon, J.M. Colvin, Strength evaluation of prosthetic check sockets, copolymer sockets, and definitive laminated sockets, J. Rehabil. Res. Dev. 49 (2012) 405–426. https://doi.org/10.1682/JRRD.2011.05.0091.

[10] C. Marcauteanu, E.T. Stoica, C. Bortun, M.L. Negrutiu, C. Sinescu, A. Tudor, Advantages of a polyethylene terephthalate glycol-modified coated with a thermoplastic polyurethane as an occlusal appliance material, Rev. Chim. 65 (2014) 734–736.

[11] D.F. Redaelli, V. Abbate, F.A. Storm, A. Ronca, A. Sorrentino, C. De Capitani, E. Biffi, L. Ambrosio, G. Colombo, P. Fraschini, D.F. Redaelli, 3D printing orthopedic scoliosis braces : a test comparing FDM with thermoforming, (2020) 1707–1720.

[12] M.H. Hassan, A.M. Omar, E. Daskalakis, Y. Hou, B. Huang, I. Strashnov, B.D. Grieve, P. Bártolo, The potential of polyethylene terephthalate glycol as biomaterial for bone tissue engineering, Polymers (Basel). 12 (2020) 1–12. https://doi.org/10.3390/polym12123045.

[13] S. Petersmann, M. Spoerk, W. Van De Steene, M. Üçal, J. Wiener, G. Pinter, F. Arbeiter, Mechanical properties of polymeric implant materials produced by extrusion-based additive manufacturing, J. Mech. Behav. Biomed. Mater. 104 (2020) 103611. https://doi.org/10.1016/j.jmbbm.2019.103611.

[14] M. Katschnig, J. Wallner, T. Janics, C. Burgstaller, W. Zemann, C. Holzer, Biofunctional glycol-modified polyethylene terephthalate and thermoplastic polyurethane implants by extrusion-based additive manufacturing for medical 3D maxillofacial defect reconstruction, Polymers (Basel). 12 (2020). https://doi.org/10.3390/POLYM12081751.

[15] D. Jiang, D.E. Smith, Anisotropic mechanical properties of oriented carbon fiber filled polymer composites produced with fused filament fabrication, Addit. Manuf. 18 (2017) 84–94. https://doi.org/10.1016/j.addma.2017.08.006.

[16] M. Mansour, K. Tsongas, D. Tzetzis, A. Antoniadis, Mechanical and Dynamic Behavior of Fused Filament Fabrication 3D Printed Polyethylene Terephthalate Glycol Reinforced with Carbon Fibers, Polym. - Plast. Technol. Eng. 57 (2018) 1715–1725. https://doi.org/10.1080/03602559.2017.1419490.

[17] P. Latko-Durałek, K. Dydek, A. Boczkowska, Thermal, Rheological and Mechanical Properties of PETG/rPETG Blends, J. Polym. Environ. 27 (2019) 2600–2606. https://doi.org/10.1007/s10924-019-01544-6.

[18] M. Kováčová, J. Kozakovičová, M. Procházka, I. Janigová, M. Vysopal, I. Černičková, J. Krajčovič, Z. Špitalský, Novel hybrid PETG composites for 3D printing, Appl. Sci. 10 (2020). https://doi.org/10.3390/app10093062.

[19] S. Valvez, A.P. Silva, P.N.B. Reis, Compressive Behaviour of 3D-Printed PETG Composites, Aerospace. 9 (2022). https://doi.org/10.3390/aerospace9030124.

[20] K. De Clerck, Filament Fabrication, (2022).

[21] L. Huang, S. An, C. Li, C. Huang, S. Wang, X. Zhang, M. Xu, J. Chen, L. Zhou, Performance of waste-paper/PETG wood-plastic composites, AIP Adv. 8 (2018). https://doi.org/10.1063/1.5026265.

[22] C. Chemistry, Bamboo Flour / Petg Composites : Compatibilizing Effect of, 53 (2019) 145–154.

[23] A.K.M.M. Alam, Q.T.H. Shubhra, G. Al-Imran, S. Barai, M.R. Islam, M.M. Rahman, Preparation and characterization of natural silk fiber-reinforced polypropylene and synthetic E-glass fiber-reinforced polypropylene composites: A comparative study, J. Compos. Mater. 45 (2011) 2301–2308. https://doi.org/10.1177/0021998311401082.

[24] Y.K. Hamidi, M.A. Yalcinkaya, G.E. Guloglu, M. Pishvar, M. Amirkhosravi, M.C. Altan, Silk as a natural reinforcement: Processing and properties of

silk/epoxy composite laminates, Materials (Basel). 11 (2018). https://doi.org/10.3390/ma11112135.

[25] H. Dou, B. Zuo, Effect of sodium carbonate concentrations on the degumming and regeneration process of silk fibroin, J. Text. Inst. 106 (2015) 311–319. https://doi.org/10.1080/00405000.2014.919065.

[26] J. Guo, R. Xiao, C. Tian, M. Jiang, Optimizing physical aging in poly(ethylene terephthalate)-glycol (PETG), J. Non. Cryst. Solids. 502 (2018) 15–21. https://doi.org/10.1016/j.jnoncrysol.2018.10.021.

[27] Y. Tsai, C.H. Fan, C.Y. Hung, F.J. Tsai, Transparent copolyester/organoclay nanocomposites prepared by in situ intercalation polymerization: Synthesis, characterization, and properties, Polym. Compos. 32 (2011) 89–96. https://doi.org/10.1002/pc.21021.

[28] M. Kattan, E. Dargent, J. Ledru, J. Grenet, Strain-induced crystallization in uniaxially drawn PETG plates, J. Appl. Polym. Sci. 81 (2001) 3405–3412. https://doi.org/10.1002/app.1797.

[29] F.A. dos Santos, G.C.V. Iulianelli, M.I.B. Tavares, Effect of microcrystalline and nanocrystals cellulose fillers in materials based on PLA matrix, Polym. Test. 61 (2017) 280–288. https://doi.org/10.1016/j.polymertesting.2017.05.028.

[30] L. Valentini, S. Bittolo Bon, L. Mussolin, N.M. Pugno, Silkworm silk fibers vs PEEK reinforced rubber luminescent strain gauge and stretchable composites, Compos. Sci. Technol. 156 (2018) 254–261. https://doi.org/10.1016/j.compscitech.2017.12.031.

[31] H.Y. Wang, Y.Y. Chen, Y.Q. Zhang, Processing and characterization of powdered silk micro- and nanofibers by ultrasonication, Mater. Sci. Eng. C. 48 (2015) 444–452. https://doi.org/10.1016/j.msec.2014.12.028.

[32] E. Frankenberg, 基因的改变NIH Public Access, Bone. 23 (2012) 1–7. https://doi.org/10.1002/jbm.b.31875.Effect.

[33] H.Y. Cheung, K.T. Lau, X.M. Tao, D. Hui, A potential material for tissue engineering: Silkworm silk/PLA biocomposite, Compos. Part B Eng. 39 (2008) 1026–1033. https://doi.org/10.1016/j.compositesb.2007.11.009.

[34] I.G. Kim, S.Y. Hong, B.O. Park, H.J. Choi, J.H. Lee, Polyphenylene ether/glycol modified polyethylene terephthalate blends and their physical characteristics, J. Macromol. Sci. Part B Phys. 51 (2012) 798–806.

https://doi.org/10.1080/00222348.2011.610207.

[35] S.I. Pirani, P. Krishnamachari, R. Hashaikeh, Optimum loading level of nanoclay in PLA nanocomposites: Impact on the mechanical properties and glass transition temperature, J. Thermoplast. Compos. Mater. 27 (2014) 1461–1478. https://doi.org/10.1177/0892705712473627.

[36] T. Chen, G. Jiang, G. Li, Z. Wu, J. Zhang, Poly(ethylene glycol-co-1,4-cyclohexanedimethanol terephthalate) random copolymers: Effect of copolymer composition and microstructure on the thermal properties and crystallization behavior, RSC Adv. 5 (2015) 60570–60580. https://doi.org/10.1039/c5ra09252c.

[37] S. Bhandari, R.A. Lopez-Anido, D.J. Gardner, Enhancing the interlayer tensile strength of 3D printed short carbon fiber reinforced PETG and PLA composites via annealing, Addit. Manuf. 30 (2019) 100922. https://doi.org/10.1016/j.addma.2019.100922.

[38] N.G. Karsli, A. Aytac, Tensile and thermomechanical properties of short carbon fiber reinforced polyamide 6 composites, Compos. Part B Eng. 51 (2013) 270–275. https://doi.org/10.1016/j.compositesb.2013.03.023.

[39] V.S. Sreenivasan, N. Rajini, A. Alavudeen, V. Arumugaprabu, Dynamic mechanical and thermo-gravimetric analysis of Sansevieria cylindrica/polyester composite: Effect of fiber length, fiber loading and chemical treatment, Compos. Part B Eng. 69 (2015) 76–86. https://doi.org/10.1016/j.compositesb.2014.09.025.

[40] S. Paszkiewicz, A. Szymczyk, D. Pawlikowska, I. Irska, I. Taraghi, R. Pilawka, J. Gu, X. Li, Y. Tu, E. Piesowicz, Synthesis and characterization of poly(ethylene terephthalate-: Co -1,4-cyclohexanedimethylene terephtlatate)-block -poly(tetramethylene oxide) copolymers, RSC Adv. 7 (2017) 41745–41754. https://doi.org/10.1039/c7ra07172h.

[41] S. Sheik, G.K. Nagaraja, K. Prashantha, Effect of silk fiber on the structural, thermal, and mechanical properties of PVA/PVP composite films, Polym. Eng. Sci. 58 (2018) 1923–1930. https://doi.org/10.1002/pen.24801.

[42] S. Sheik, G.K. Nagaraja, J. Naik, R.F. Bhajanthri, Development and characterization study of silk fibre reinforced poly(vinyl alcohol) composites, Int. J. Plast. Technol. 21 (2017) 108–122. https://doi.org/10.1007/s12588-017-9174-7.

[43] P. Science, E. Group, C.E. Division, C r y s t a l l i z a t i o n b e h a v i o u r of a

 doi:10.20944/preprints202209.0144.v1

r o m a t i c c o p o l y e s t e r m o d i f i e d w i t h a l i c y c l i c diol*, 22 (1986) 67–70.

[44] G. Li, H. Liu, T. Li, J. Wang, Surface modification and functionalization of silk fibroin fibers/fabric toward high performance applications, Mater. Sci. Eng. C. 32 (2012) 627–636. https://doi.org/10.1016/j.msec.2011.12.013.

[45] Y.Q. Zhao, H.Y. Cheung, K.T. Lau, C.L. Xu, D.D. Zhao, H.L. Li, Silkworm silk/poly(lactic acid) biocomposites: Dynamic mechanical, thermal and biodegradable properties, Polym. Degrad. Stab. 95 (2010) 1978–1987. https://doi.org/10.1016/j.polymdegradstab.2010.07.015.

[46] M.T. Ramesan, V.K. Athira, P. Jayakrishnan, C. Gopinathan, Preparation, characterization, electrical and antibacterial properties of sericin/poly(vinyl alcohol)/poly(vinyl pyrrolidone) composites, J. Appl. Polym. Sci. 133 (2016) 1–10. https://doi.org/10.1002/app.43535.

[47] D.U. Shah, D. Porter, F. Vollrath, Can silk become an effective reinforcing fibre? A property comparison with flax and glass reinforced composites, Compos. Sci. Technol. 101 (2014) 173–183. https://doi.org/10.1016/j.compscitech.2014.07.015.